Supplement of

Dynamic upper-ocean processes enhance mesopelagic carbon export of zooplankton fecal pellets in the southern South China Sea

Ruitong Wu et al.

Correspondence: Zhifei Liu (lzhifei@tongji.edu.cn)

Contents of this file

Introduction

This supplement contains 8 figures, 1 text, and 1 table. Figures S1 to S6 show the typical optical micrographs of zooplankton fecal pellets collected from the UP trap (500 m water depth) at Mooring TJ-S in the southern South China Sea (SCS) from August 2022 to May 2023. These zooplankton fecal pellets were photographed at 8X and 50X magnifications, respectively. Figure S7 shows the biovolume distribution and average values of three types of fecal pellets at TJ-S (500 m). Figure S8 displays correlations between mean individual pellet biovolume and FPN, PP, SST, and nitrate concentration across different types of fecal pellets. Text S1 explains the variations in regional zooplankton community and fecal pellet biovolume in more detail. Table S1 includes flux data of zooplankton fecal pellets and particulate organic carbon of time-series sediment trap samples from 2022–2023 at Mooring TJ-S.

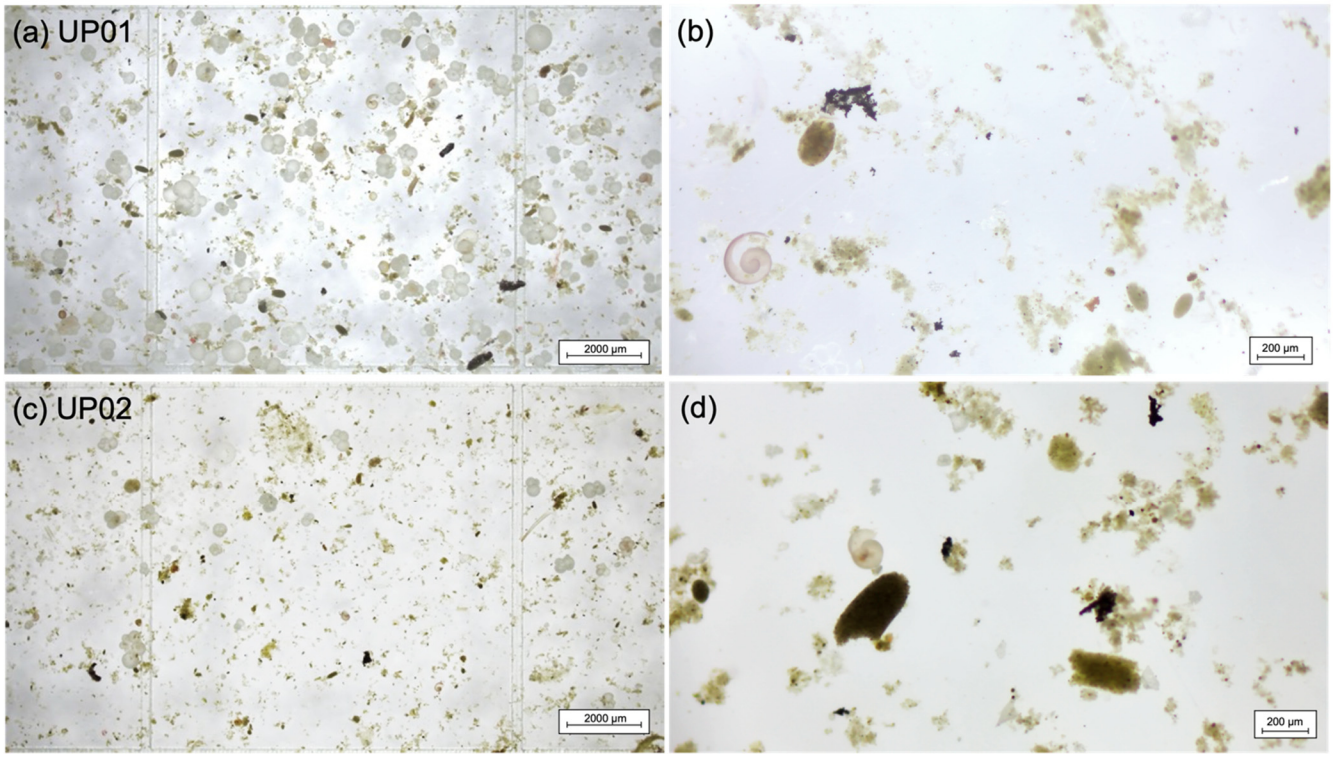

Figure S1. Zooplankton fecal pellets of Samples TJ-S22-UP01 (**a-b**) and TJ-S22-UP02 (**c-d**) at 500 m at the sediment trap mooring TJ-S in the southern SCS. (**a**) Pellets at 8X magnification, sample fraction: 1/4; (**b**) pellets at 50X magnification, sample fraction: 1/4; (**c**) pellets at 8X magnification, sample fraction: 1/8; (**d**) pellets at 50X magnification, sample fraction: 1/8.

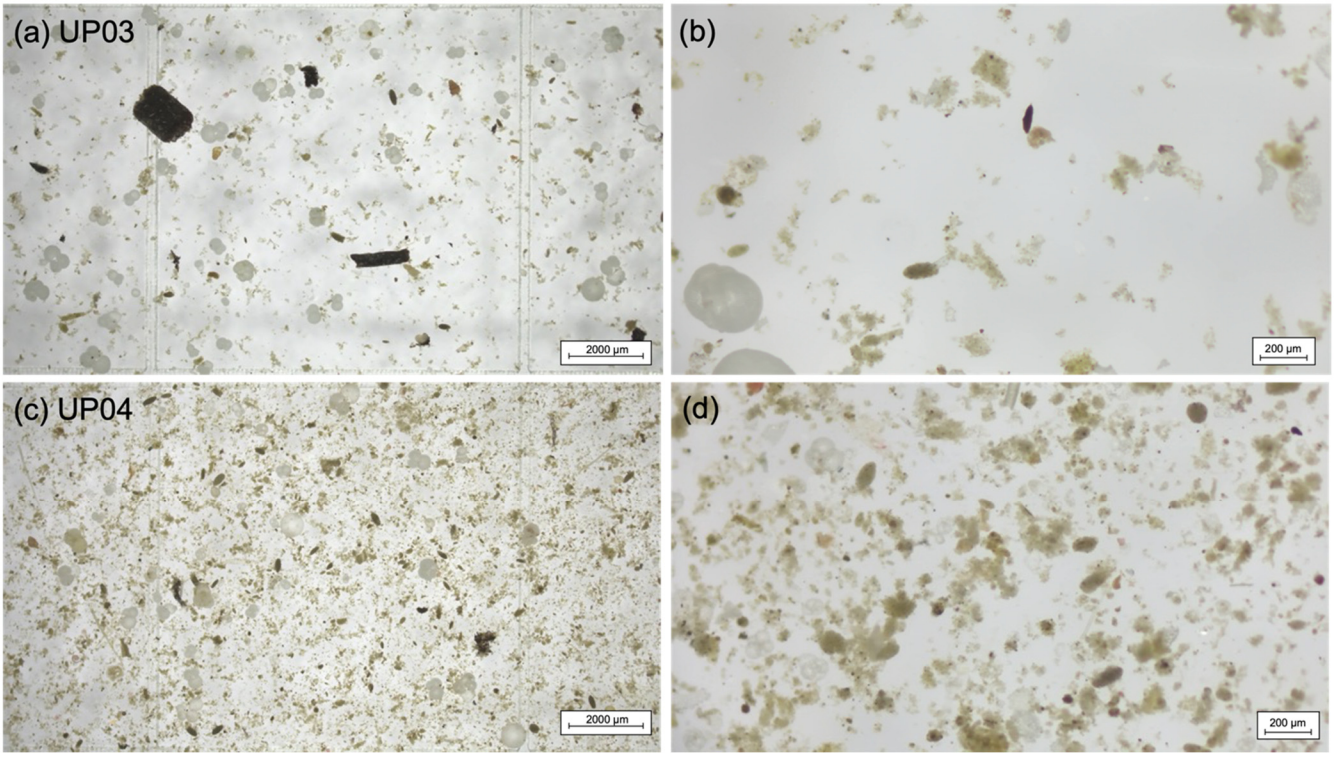

Figure S2. Zooplankton fecal pellets of Samples TJ-S22-UP03 (**a-b**) and TJ-S22-UP04 (**c-d**) at 500 m at the sediment trap mooring TJ-S in the southern SCS. (**a**) Pellets at 8X magnification, sample fraction: 1/4; (**b**) pellets at 50X magnification, sample fraction: 1/4; (**c**) pellets at 8X magnification, sample fraction: 1/8; (**d**) pellets at 50X magnification, sample fraction: 1/8.

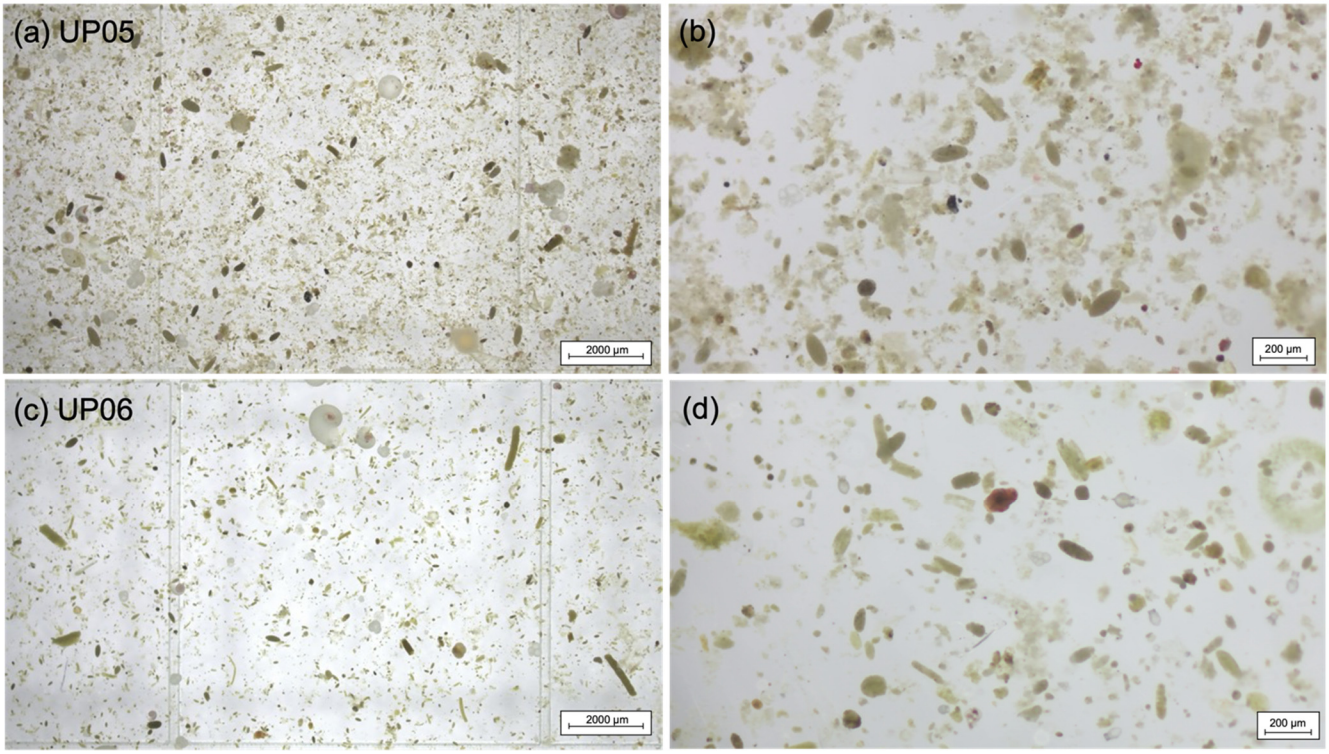

Figure S3. Zooplankton fecal pellets of Samples TJ-S22-UP05 (**a-b**) and TJ-S22-UP06 (**c-d**) at 500 m at the sediment trap mooring TJ-S in the southern SCS. (**a**) Pellets at 8X magnification, sample fraction: 1/12; (**b**) pellets at 50X magnification, sample fraction: 1/12; (**c**) pellets at 8X magnification, sample fraction: 1/64; (**d**) pellets at 50X magnification, sample fraction: 1/64.

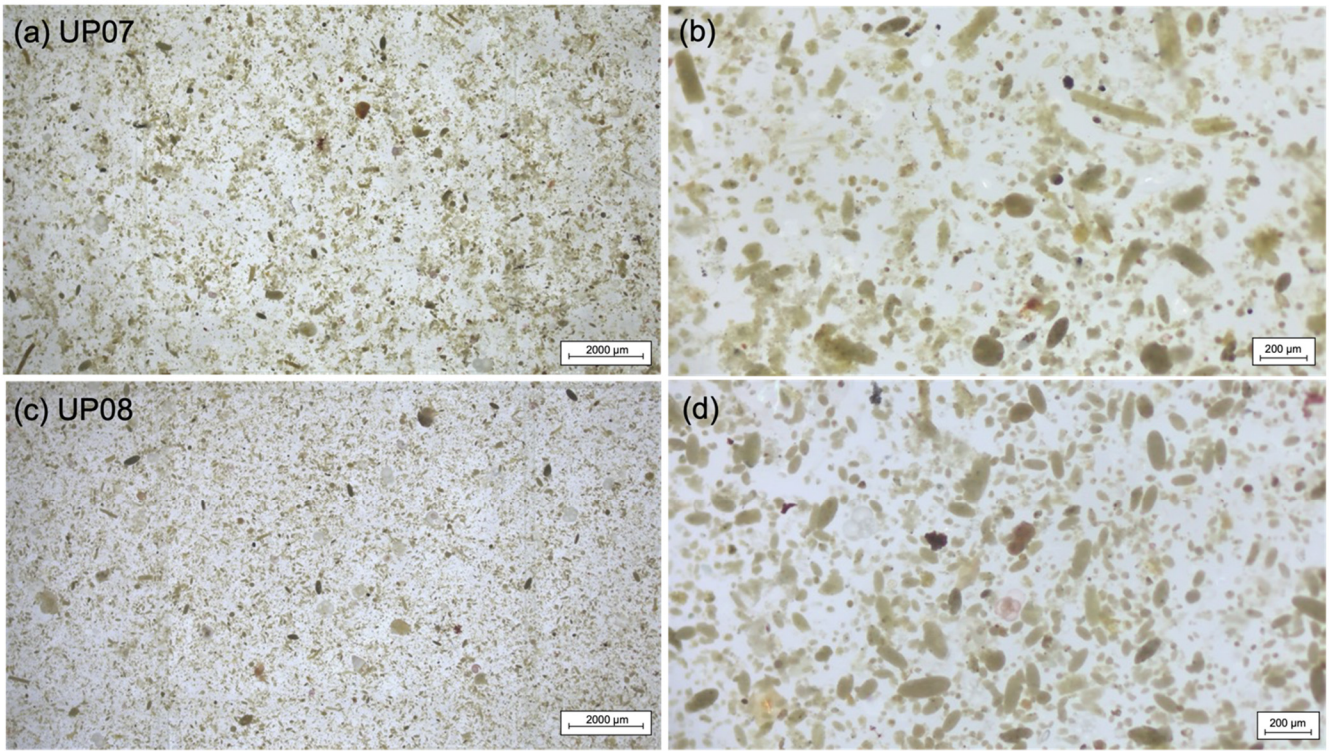

Figure S4. Zooplankton fecal pellets of Samples TJ-S22-UP07 (**a-b**) and TJ-S22-UP08 (**c-d**) at 500 m at the sediment trap mooring TJ-S in the southern SCS. (**a**) Pellets at 8X magnification, sample fraction: 1/8; (**b**) pellets at 50X magnification, sample fraction: 1/8; (**c**) pellets at 8X magnification, sample fraction: 1/12; (**d**) pellets at 50X magnification, sample fraction: 1/12.

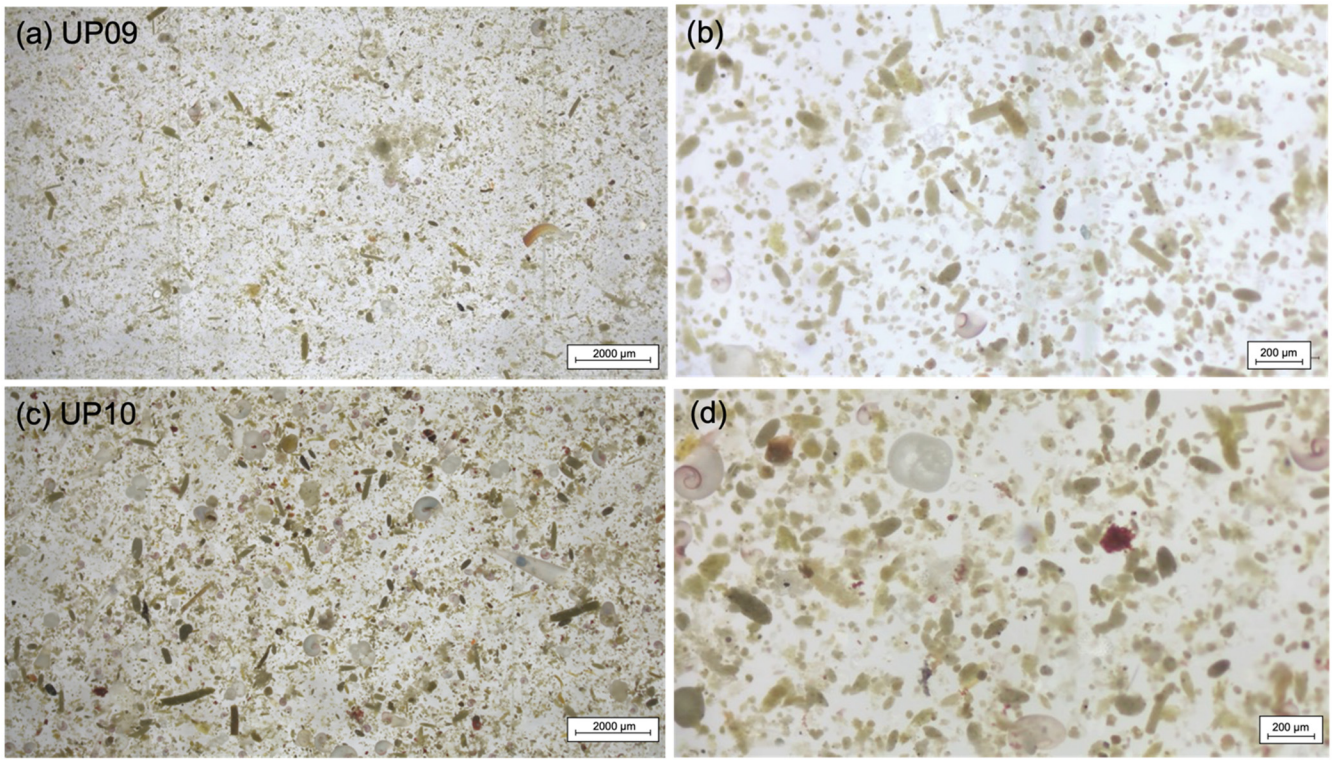

Figure S5. Zooplankton fecal pellets of Samples TJ-S22-UP09 (**a-b**) and TJ-S22-UP10 (**c-d**) at 500 m at the sediment trap mooring TJ-S in the southern SCS. (**a**) Pellets at 8X magnification, sample fraction: 1/32; (**b**) pellets at 50X magnification, sample fraction: 1/32; (**c**) pellets at 8X magnification, sample fraction: 1/8; (**d**) pellets at 50X magnification, sample fraction: 1/8.

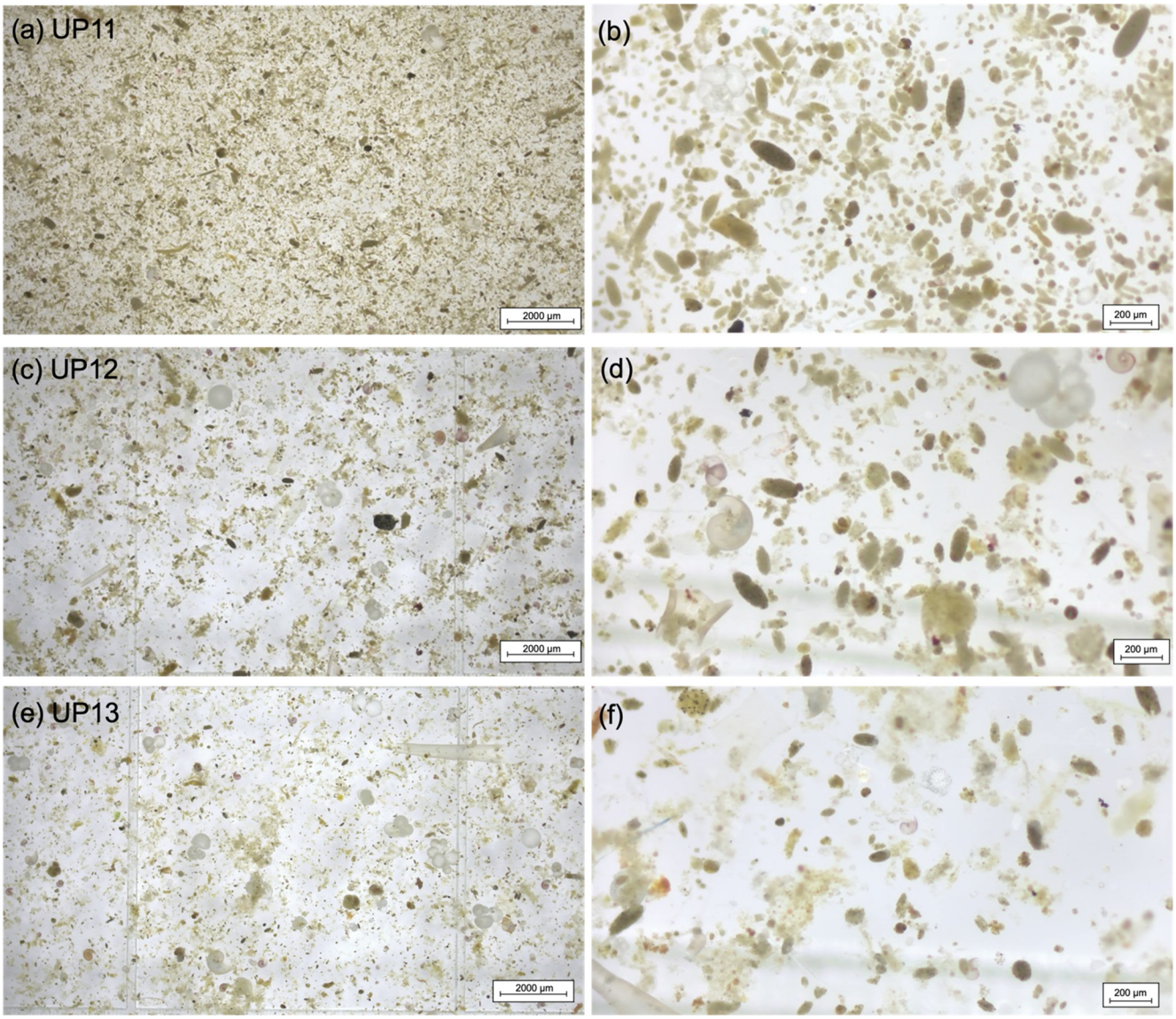

Figure S6. Zooplankton fecal pellets of Samples TJ-S22-UP11 (**a-b**), TJ-S22-UP12 (**c-d**) and TJ-S22-UP13 (**e-f**) at 500 m at the sediment trap mooring TJ-S in the southern SCS. (**a**) Pellets at 8X magnification, sample fraction: 1/48; (**b**) pellets at 50X magnification, sample fraction: 1/48; (**c**) pellets at 8X magnification, sample fraction: 1/8; (**d**) pellets at 50X magnification, sample fraction: 1/8; (**e**) pellets at 8X magnification, sample fraction: 1/16; (**f**) pellets at 50X magnification, sample fraction: 1/16.

Text S1. Variations in the regional zooplankton community and fecal pellet biovolume

The morphological characteristics of zooplankton fecal pellets vary among different species. Thus, the relative abundance of different fecal pellets in sediment trap samples may serve as a proxy for regional zooplankton community structure (Wilson et al., 2008). Our quantitative analysis of fecal pellets at 500 m reveals a remarkably stable annual composition (Fig. 3c): In 85 % of all the cases, ellipsoidal pellets dominated (48 % ± 5.5 %), followed by spherical (38 % ± 4.4 %) and cylindrical pellets (15 % ± 4.4 %). In 15 % of all cases, the abundance of ellipsoidal pellets fell slightly below spherical pellets (- 4 %) but still has a distinct contribution (> 37 %). This consistent pattern implies temporal stability in the zooplankton community structure in the research area, as evidenced by proportional fluctuations in all pellet types during periods of high and low fluxes. While the numerical proportions remained stable, we observed significant temporal variability in the carbon contribution of different types of fecal pellets (Fig. 3f). In 54 % of all observations, cylindrical pellets contributed the most (38 % ± 10.3 %), and contribution of cylindrical pellets fell below ellipsoidal pellets (35.5 % ± 6.9 %) in 31 % of the observations and was even lower than spherical pellets (26.7 % ± 7.5 %) in 15 % of the observations. This discrepancy between the numerical and carbon contribution suggests dynamic changes in individual pellet volume and carbon content that cannot be explained by abundance alone. Since the carbon content is calculated by fecal pellet biovolume and carbon-volume conversion factor, this result provides insights into the temporal variation of the size of individual fecal pellet. Analysis of individual fecal pellet biovolume in the upper water column revealed synchronous seasonal patterns across all three morphotypes, characterized by high carbon content in summer and low carbon content during winter (Fig. S7). Negative relationships between fecal pellet biovolume, surface nitrate, FPN, and primary productivity in the upper volume (100 m) were identified in our samples (Fig. S8).

This result, however, contradicts previous studies on fecal pellet biovolumes. The size of fecal pellets is believed to be primarily determined by the size of their producers and can be further influenced by a complex series of bio-geochemical processes, including diet (Besiktepe and Dam, 2002), food concentration (Breteler et al., 1982), and feeding efficiency (Atkinson et al., 2012). Lab experiments have demonstrated a tight coupling relationship between ingestion and defecation in the copepod *Acartia tonsa* (Besiktepe and Dam, 2002). Both diet composition and food concentration have significant effects on grazing dynamics, with ingestion rate, fecal pellet production rate, and pellet volume all exhibiting strong dependence on these factors. In their research, copepods achieved the largest pellet volume under the diatom diet, with pellet volume increasing curvilinearly with increasing food concentration (Besiktepe and Dam, 2002). Previous studies of marine copepods observed high absorption efficiency during periods of low feeding rates, leading to the production of smaller, densely packed pellets, whereas good feeding conditions often result in larger, slow-sinking pellets and greater potential for disaggregation or remineralization (Mitra and Flynn, 2007; Thor and Wendt, 2010; Steinberg and Landry, 2017).

In our studies, we assume that the food concentration at the mooring site is positively related to surface primary productivity and nutrient concentration. However, the negative relationship between primary productivity, nitrate concentration, and pellet volume suggests that zooplankton dynamics in the region do not strictly follow established feeding patterns (Fig. S8). The pellets enumerated and measured in our photos show clear shapes and edges. Thus, the fragmentation of larger fecal pellets

cannot be an explanation. We hypothesize that this anomaly probably arises from the complexity of the zooplankton community and the instability of diets and food concentration in the study area. Notably, a positive relationship between pellet biovolume and SST was observed (Fig. S8). The temperature-size effect on marine copepod species has been widely recognized in many studies and has also been proven by experiments under controlled environmental conditions (Breteler et al., 1982). Thus, we believe that the variations of fecal pellet volume at station TJ-S largely depend on zooplankton size instead of food concentration, and the changes in absorption efficiency have no effect on pellet size.

While the three morphotypes generally show synchronous pellet volume variations, notable asynchronies occur during specific events. In late November, volumes of ellipsoidal and spherical pellets show concurrent increases (by 32 % and 28 %, respectively), whereas cylindrical pellets exhibit no significant change ($\Delta < 5$ %, $p = 0.42$). This discrepancy indicates different responses of zooplankton communities to climate events, or there might be a competitive exclusion of cylindrical pellet producers in the community structure. In early March, we observed a significant increase in the biovolume of all three types of pellets. Intriguingly, this increase temporarily coincides with one of the nutrient peaks in winter. This seems to support the theories of food concentration and assimilation efficiency; however, no pellet volume increase was observed during other nutrient peaks that occurred in January and February. Overall, the observed individual FPC variations underscore the complexity of the response of the zooplankton community to environmental factors and food availability.

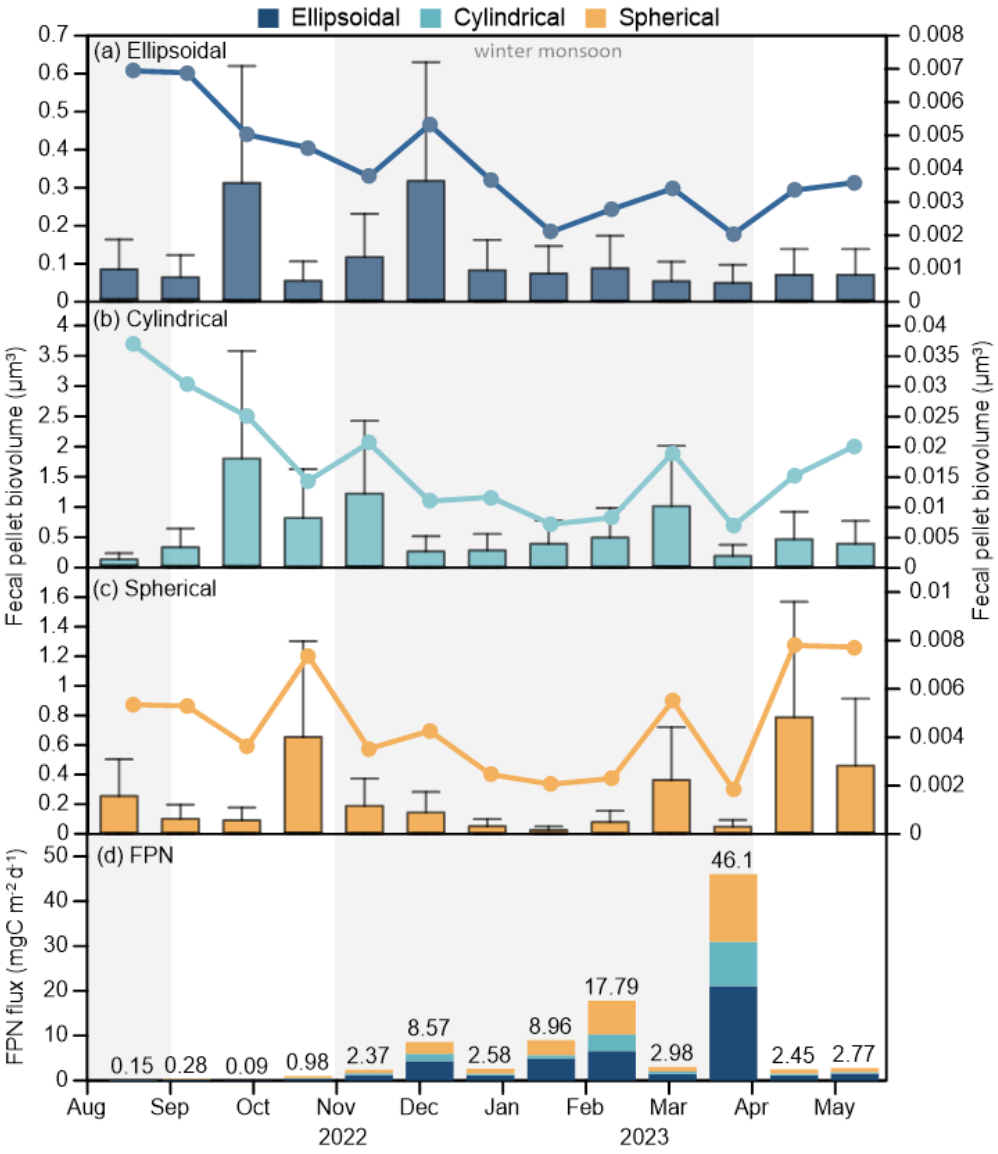

110 **Figure S7.** Biovolume distribution and average values of three types of fecal pellets at TJ-S (500 m) in the southern SCS. (**a**) Ellipsoidal; (**b**) cylindrical; (**c**) spherical. (**d**) FPN. Grey bars indicate monsoon periods as in Fig 3.

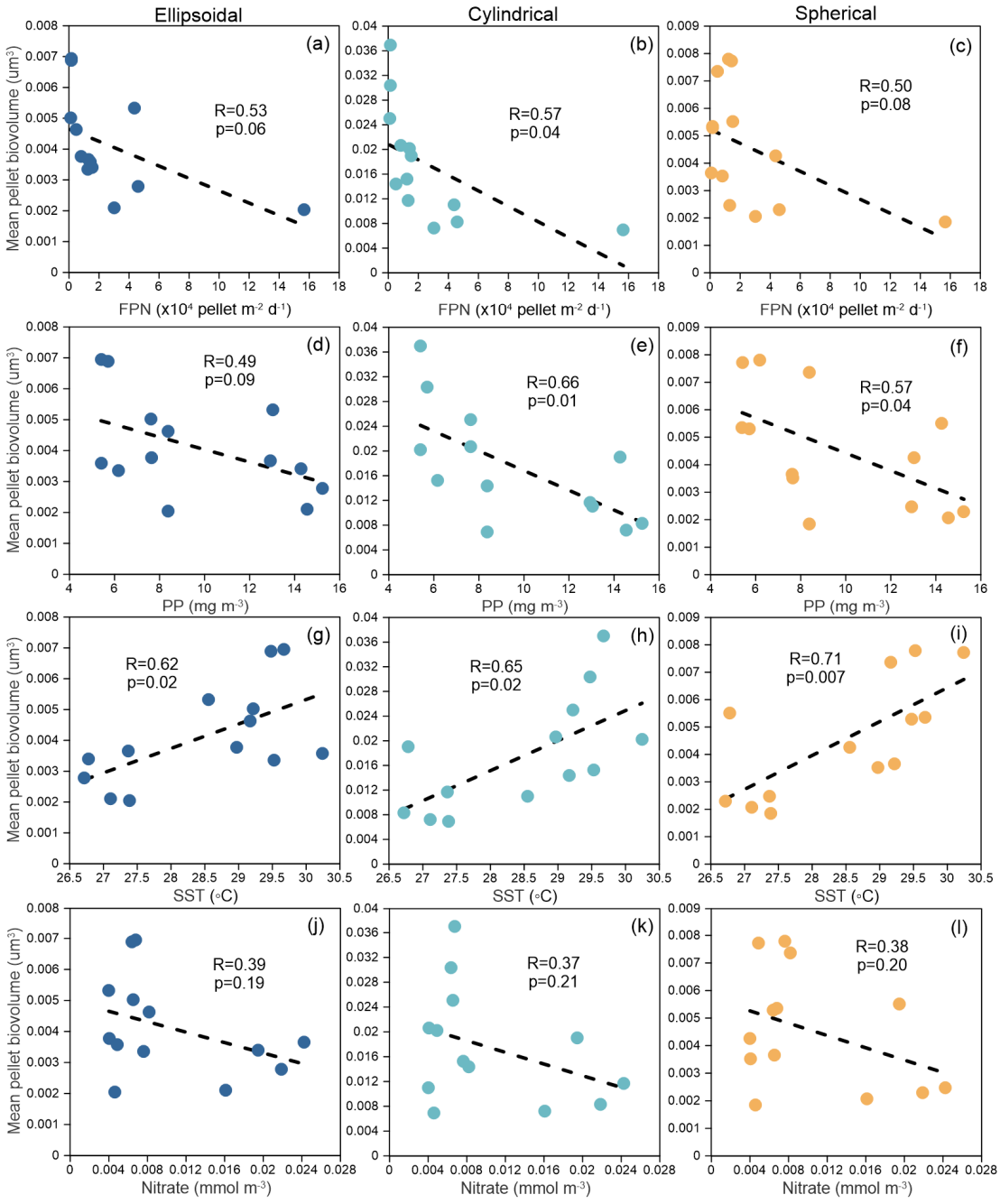

Figure S8. Correlations between mean individual pellet biovolume and FPN, PP, SST and nitrate concentration across different types of fecal pellets. (**a-c**) biovolume and FPN; (**d-f**) biovolume and PP; (**g-i**) biovolume and SST; (**j-l**) biovolume and nitrate. Dashed lines indicate linear correlation with a coefficient of R.

Table S1. Flux data of zooplankton fecal pellets and particulate organic carbon of time-series sediment trap samples during 2022–2023 at Mooring TJ-S in the SCS

No.	Sample name	Date start	Date end	Total mass flux (mg m^{-2} d^{-1})	POC content (%)	POC flux (mg C m^{-2} d^{-1})	Fecal pellet numerical flux (pellets m^{-2} d^{-1})	Ellipsoidal pellet numerical flux (pellets m^{-2} d^{-1})	Cylindrical pellet numerical flux (pellets m^{-2} d^{-1})	Spherical pellet numerical flux (pellets m^{-2} d^{-1})	Fecal pellet carbon flux (mg C m^{-2} d^{-1})	Ellipsoidal pellet carbon flux (mg C m^{-2} d^{-1})	Cylindrical pellet carbon flux (mg C m^{-2} d^{-1})	Spherical pellet carbon flux (mg C m^{-2} d^{-1})	FPC/ POC ratio (%)
1	TJ-S22-UP01	2022-08-09	2022-08-25	16.41	1.40	0.23	1526	854	107	565	0.05	0.02	0.01	0.01	20.1
2	TJ-S22-UP02	2022-08-26	2022-09-16	11.77	2.46	0.29	2781	1249	331	1201	0.09	0.03	0.04	0.02	31.0
3	TJ-S22-UP03	2022-09-17	2022-10-08	9.84	0.79	0.08	937	430	140	367	0.03	0.01	0.02	0.00	42.6
4	TJ-S22-UP04	2022-10-09	2022-10-30	26.21	3.35	0.88	9825	4033	1291	4501	0.17	0.06	0.04	0.07	19.3
5	TJ-S22-UP05	2022-10-31	2022-11-21	28.75	4.59	1.32	23746	12189	3554	8003	0.40	0.16	0.15	0.09	30.2
6	TJ-S22-UP06	2022-11-22	2022-12-13	244.44	4.65	11.38	85682	43107	16326	26249	1.61	0.72	0.55	0.34	14.2
7	TJ-S22-UP07	2022-12-14	2023-01-04	65.53	4.55	2.98	25799	11364	4035	10400	0.37	0.13	0.14	0.09	12.2
8	TJ-S22-UP08	2023-01-05	2023-01-26	185.27	2.49	4.61	89632	49324	6951	33357	0.77	0.36	0.16	0.24	16.6
9	TJ-S22-UP09	2023-01-27	2023-02-17	268.91	3.53	9.50	177944	65247	37521	75176	2.14	0.64	0.94	0.57	22.5
10	TJ-S22-UP10	2023-02-18	2023-03-11	87.18	4.39	3.83	29823	14696	4957	10170	0.58	0.18	0.25	0.15	15.2
11	TJ-S22-UP11	2023-03-12	2023-04-02	513.66	3.11	15.97	461018	210832	98733	151453	4.62	1.53	2.19	0.90	28.9
12	TJ-S22-UP12	2023-04-03	2023-04-24	56.99	4.90	2.79	24467	11630	3422	9415	0.49	0.14	0.18	0.18	17.6
13	TJ-S22-UP13	2023-04-25	2023-05-17	84.64	6.45	5.46	27729	15065	3111	9553	0.55	0.19	0.18	0.18	10.0

References cited in supplementary material:

Atkinson, A., Schmidt, K., Fielding, S., Kawaguchi, S., and Geissler, P. A.: Variable food absorption by Antarctic krill: Relationships between diet, egestion rate and the composition and sinking rates of their fecal pellets, Deep Sea Res. Part II, 59-60, 147–158, https://doi.org/10.1016/j.dsr2.2011.06.008, 2012.

Besiktepe, S. and Dam, H.: Coupling of ingestion and defecation as a function of diet in the calanoid copepod Acartia tonsa, Mar. Ecol. Prog. Ser., 229, 151–164, https://doi.org/10.3354/meps229151, 2002.

Breteler, W. K., Fransz, H. G., and Gonzalez, S. R.: Growth and development of four calanoid copepod species under experimental and natural conditions, Neth. J. Sea Res., 16, 195–207, https://doi.org/10.1016/0077-7579(82)90030-8, 1982.

Mitra, A. and Flynn, K. J.: Importance of interactions between food quality, quantity, and gut transit time on consumer feeding, growth, and trophic dynamics, Am. Nat., 169, 632–646, https://doi.org/10.1086/513187, 2007.

Steinberg, D. K. and Landry, M. R.: Zooplankton and the Ocean Carbon Cycle, Ann Rev Mar Sci, 9, 413–444, https://doi.org/10.1146/annurev-marine-010814-015924, 2017.

Thor, P. and Wendt, I.: Functional response of carbon absorption efficiency in the pelagic calanoid copepod Acartia tonsa, Limnol. Oceanogr., 55, 1779–1789, https://doi.org/10.4319/lo.2010.55.4.1779, 2010.

Wilson, S. E., Steinberg, D. K., and Buesseler, K. O.: Changes in fecal pellet characteristics with depth as indicators of zooplankton repackaging of particles in the mesopelagic zone of the subtropical and subarctic North Pacific Ocean, Deep Sea Res. Part II, 55, 1636–1647, https://doi.org/10.1016/j.dsr2.2008.04.019, 2008.